Polyhedron 85 (2015) 60–68

Contents lists available at ScienceDirect

Polyhedron

journal homepage: www.elsevier.com/locate/poly

Side-chain-modulated supramolecular assembly between CuX_2 (X = Cl, Br) and quasi-planar π-conjugated organic synthons of 1, 3, 5-tris(2-alkylthiolpyrimidinyl)benzene: Crystal structures and conductive properties

Hai-Bin Zhu [a,*], Yan-Fang Wu [a], Ge Zhang [a], Yong-Bing Lou [a,*], Jun Hu [b]

[a] School of Chemistry and Chemical Engineering, Southeast University, Nanjing 211189, China
[b] Coordination Chemistry Institute, Nanjing University, Nanjing 210093, China

ARTICLE INFO

Article history:
Received 24 July 2014
Accepted 20 August 2014
Available online 27 August 2014

Keywords:
π-conjugated
Quasi-planar
Side-chain-effect
Crystal structures
Conductivity

ABSTRACT

A class of π-conjugated organic synthons, namely 1, 3, 5-tris(2-alkylthiolpyrimidinyl)benzene (**TMPB**: alkyl = Me; **TEPB**: alkyl = Et; **TPPB**: alkyl = n-Pr) was designed and prepared, which only differ in the length of linear side chain. It was found that these organic synthons can keep a quasi-planar conformation even coordinated to metal ions due to intramolecular C–H···N hydrogen bonds. Assembly of these organic synthons with CuX_2 (X = Cl, Br) generated four coordination polymers: $[(\mathbf{TPPB})CuCl_2]_n$ (**1**), $\{[(\mathbf{TMPB})CuCl_2]\cdot H_2O\}_n$ (**2**), $[(\mathbf{TPPB})CuBr_2]_n$ (**3**), $[(\mathbf{TEPB})CuBr_2]_n$ (**4**), among which **1**–**3** exhibit one-dimensional coordination ribbon structure and **4** shows a two-dimensional wave-like coordination network. Although **1**–**3** exhibit similar assembly hierarchy going from 1-D ribbon through 2-D supramolecular layer to 3-D supramolecular architecture, the side-chain-effect can be clearly seen which modulates intra-chain or inter-chain Cu···Cu distance; inter-chain C–H···S supramolecular interactions and even the co-existence of guest water molecules. The room-temperature direct-current (dc) conductivity of **1**–**4** is measured about 9.6×10^{-12} S cm^{-1}, 2.9×10^{-9} S cm^{-1}, 2.6×10^{-12} S cm^{-1} and 5.7×10^{-11} S cm^{-1}, respectively, wherein the highest electronic conduction of **2** is assumed to be pertinent to the existence of unique inter-chain C–H···S interactions. Furthermore, the complex impedance technique reveals that **2** exhibits a alternate-current (ac) conductivity of 4.3×10^{-6} S cm^{-1} at room temperature, which almost decreases linearly with the rising temperature. The higher ac conductivity of **2** against its dc conductivity is assumed to be largely contributed by proton-conduction as the matter of fact that there exist in **2** guest water molecules and water-molecule-associated O–H···Cl hydrogen bonding network. The unusual temperature-dependent ac conductivity of **2** is possibly due to the temperature-sensitive O–H···Cl hydrogen bonding network, which is responsible for proton transporting.

1. Introduction

In recent years, electrically conducting coordination polymers [1–3] especially those with permanent porosity (e.g. MOFs = metal–organic-frameworks) [4–9] have stimulated tremendous interest from the academic community largely due to their great potential in solid-state nanoelectronic devices [10]. The key to gain electronic conduction for coordination polymers is how to build electron transporting pathway at the molecular level. To address this critical issue, two strategies have been envisioned, namely "through-space" and "through-bond", wherein one realizes the electron-flowing passage through close π-stacking interactions between redox-active organic component [11–14], and the other facilitates electron-mobilization *via* metal–ligand coordination bond generally involving either metal/ligand $p_{\pi^*} - d_\pi$ conjugation or mixed-valence of metal ions [15–19]. Amongst various conductive coordination polymers, those in one dimension should be the simplest ones which can be comparable to the mature organic conducting polymer [20–21]. Imagining a picture of an ideal organic conducting polymer, it should have π-conjugated backbone keeping almost planar conformation to maximize π-delocalization. Besides, it is worth noting that electrical properties of organic conducting polymers depend on not only the molecular structure but

* Corresponding authors.
E-mail addresses: zhuhaibin@seu.edu.cn (H.-B. Zhu), yjs_seu@163.com (Y.-F. Wu), 810179386@qq.com (G. Zhang), lou@seu.edu.cn (Y.-B. Lou), hjun@nju.edu.cn (J. Hu).

http://dx.doi.org/10.1016/j.poly.2014.08.051
0277-5387/

also the molecular packing. In order to modulate the molecular assembly of organic conducting polymer chain, side-chain-effect has been proven an effective tool, that is, varying the side chain attached polymeric backbone can tune the molecular ordering [22–25]. Moreover, S···S and C–H···S contacts have been found to be two major forces in organic conductor, which has been proposed as a crystal engineering tool in design of new organic conducting materials [26]. Inspired by these designing elements for organic conducting materials, we conceive that constructing one-dimensional conductive coordination polymer might take into account these points from the designing perspective: (i) organic component: large planar π-conjugated organic sulfur-containing skeleton modified by side chains; (ii) inorganic component: redox-active metal ion giving rise to MLCT or LMCT transition in expectation of improving metal-to-ligand electronic communication. As a proof of concept, we have previously designed a π-conjugated organic synthon **TEPB** (**TEPB** = 1, 3, 5-tris(2-ethylthiopyrimidinyl)benzene) which maintains a quasi-planar conformation due to intramolecular C–H···N hydrogen bonds even coordinated to metal ions. Assembly of **TEPB** with $CuCl_2$ resulted in a one-dimensional flat coordination polymeric chain of $\{[\mathbf{TEPB})CuCl_2].H_2O\}_n$ interacting with each other *via* C–H···S supramolecular interactions, which shows a room-temperature ac conductivity of 5.90×10^{-9} S cm^{-1} [27]. In this work, we investigate the side chain effect on supramolecular assembly between CuX_2 (X = Cl, Br) with 1, 3, 5-tris(2-alkylthiolpyrimidinyl)benzene (alkyl = Me, Et, n-Pr), wherein new organic synthons of **TMPB** (alkyl = Me) and **TPPB** (alkyl = n-Pr) have been synthesized for this purpose (Scheme 1). Supramolecular assembly of CuX_2 (X = Cl, Br) with 1, 3, 5-tris(2-alkylthiolpyrimidinyl)benzene (alkyl = Me, Et, Pr) resulted in four coordination polymers: $[(\mathbf{TPPB})CuCl_2]_n$ (**1**), $\{[(\mathbf{TMPB})CuCl_2]\cdot H_2O\}_n$ (**2**), $[(\mathbf{TPPB})CuBr_2]_n$ (**3**) and $[(\mathbf{TEPB})CuBr_2]_n$ (**4**), among which **1**–**3** exhibit one-dimensional coordination chain structure and **4** shows a two-dimensional network. By structural comparison of **1**–**4**, it reveals that the side chain has an important effect on their assembly structures, which further influences their conductive properties.

2. Experimental

2.1. Materials and measurements

All solvents and reagents of analytical grade were used as received without prior purification. IR spectra were recorded with a Thermo Scientific Nicolet 5700 FT-IR spectrophotometer with KBr pellets in the 400–4000 cm^{-1} region. ^{1}H-NMR spectra were recorded with a Bruker AVANCE-500 spectrometer. Electrospray ionization (ESI) mass spectra were recorded with a Finnigan MAT SSQ 710 mass spectrometer in the scan range 100–1200 amu. Elemental analyses for C, H and N were performed on a CHN-O-Rapid analyzer and an Elementar Vario MICRO analyzer. The solid-state UV–Vis absorption spectra were recorded with a Shimadzu UV-2450UV–Vis spectrophotometer. The conducting properties of

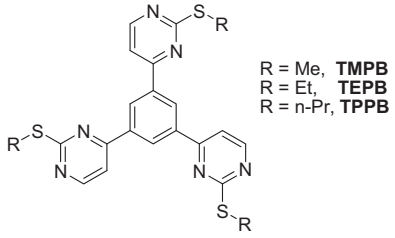

Scheme 1. Organic Synthons of 1, 3, 5-tris(2-alkylthiolpyrimidinyl)benzene (alkyl = Me, Et, n-Pr).

1–**4** were measured on pressed powder pellet samples sandwiched by a square brass electrode (10×10 mm^2) with a CHI660D (Chenghua, Shanghai) electrochemistry workstation. The thicknesses of the pellet samples of **1**–**4** are 0.72, 1.38, 0.98 and 0.98 mm, respectively.

2.2. Syntheses of *TMPB* and *TPPB*

TMPB and **TPPB** were prepared in a similar procedure to **TEPB** [27], only differing in the alkylating reagent (**TMPB**: CH_3I; **TPPB**: *n*-C_3H_7I).

TMPB: Yield 35%. IR(KBr, cm^{-1}):, 2927w, 1552s, 1444s, 1415m, 1388s, 1340m, 1311m, 1272w, 1207m, 1183m, 1126w, 971w, 904w, 820m, 790w, 772w, 741w, 719w, 677w, 636m, 628m. ^{1}H NMR($CDCl_3$/TMS, 500MHz, ppm): δ 8.93(s, 3H), 8.65(d, 3H), 7.52(d, 3H), 2.60(s, 9H). MS (ESI): *m*/*z* (%) = 451 (100) $[M+H]^+$. *Anal.* Calc. for $C_{21}H_{18}N_6S_3$: C, 55.97; H, 4.03; N, 18.65. Found: C, 55.81; H, 3.95; N, 18.54%.

TPPB: Yield 32%. IR(KBr, cm^{-1}): 2964m, 2925m, 2871w,1554vs, 1453s, 1394s, 1358w, 1328s, 1270w, 1202s, 1182 m, 1119w, 1065w, 899 m, 822s, 774w, 737m, 717m, 682w, 632m, 482w. ^{1}H NMR($CDCl_3$/TMS, 300 MHz, ppm): δ 8.87 (s, 3H), 8.62 (d, 3H), 7.49 (d, 3H), 3.24 (t, 6H), 1.86 (m, 6H), 1.11(m, 9H). MS (ESI): *m*/*z* (%) = 535 (100) $[M+H]^+$. *Anal.* Calc. for $C_{27}H_{30}N_6S_3$: C, 60.64; H, 5.65; N, 15.72. Found: C, 60.92; H, 5.58; N, 15.66%.

2.3. Preparation of *1–4*

For **1**, **3** and **4**: A CH_3OH solution (5.0 mL) containing CuX_2 (X = Cl or Br) (0.1 mmol) was carefully layered above a CH_2Cl_2 solution (5.0 mL) of **TMPB** or **TPPB** (0.05 mmol). Crystals of **1**, **3** and **4** were formed over a period of 3–4 weeks. Single crystal suitable for X-ray diffraction analysis was selected from the resultant crystals. For **2**, the only difference is that an intermediate buffer layer (4 mL) containing MeOH and CH_2Cl_2 in 1:1 volume ratio was placed between the metal-rich solution layer and ligand-rich solution layer.

$[(\mathbf{TPPB})CuCl_2]_n$ (**1**) (deep green): Yield 43% (based on **TPPB**). IR (KBr, cm^{-1}): 3234w, 2962w, 1638w, 1618s, 1570m, 1556m, 1401m, 1364m, 1328 m, 1263w, 1203m, 1180w, 1090w, 834m, 771w, 733w, 637w,482w. *Anal.* Calc. for $C_{27}H_{30}N_6S_3CuCl_2$: C, 48.46; H, 4.52; N, 12.56. Found: C, 48.52; H, 4.68; N, 12.86%.

$\{[(\mathbf{TMPB})CuCl_2].H_2O\}_n$ (**2**) (deep green): Yield 43% (based on **TMPB**). IR (KBr, cm^{-1}): 3084w, 2930w, 1635w, 1571vs, 1553vs, 1417s, 1385s, 1347s, 1309m, 1263m, 1205m, 1183m, 1132w, 1093w, 1013w, 976w, 902w, 837m, 795w, 771w, 739w, 715w, 739w, 682w, 655m, 636m. *Anal.* Calc. for $C_{21}H_{20}N_6OS_3CuCl_2$: C, 41.82; H, 3.34; N, 13.94. Found: C, 41.72; H, 3.58; N, 13.76%.

$[(\mathbf{TPPB})CuBr_2]_n$ (**3**) (deep green): Yield 48% (based on **TPPB**). IR (KBr, cm^{-1}): 3436w, 2961w, 2928w, 2870w, 1570vs, 1450w, 1421s, 1361s, 1326m, 1264w, 1204s, 1179m, 1129w, 1089w, 1008w, 895w, 832m, 772w, 732w, 681w, 637w. *Anal.* Calc. for $C_{27}H_{30}N_6S_3CuBr_2$: C, 42.78; H, 3.99; N, 11.09. Found: C, 42.42; H, 3.78; N, 11.35%.

$[(\mathbf{TEPB})CuBr_2]_n$ (**4**) (deep blue): Yield 55% (based on **TEPB**). IR (KBr, cm^{-1}): 3437m, 3080w, 3056w, 2971w, 2929w, 1571vs, 1445w, 1419s, 1384m, 1361m, 1344m, 1264m, 1206m, 1181m, 1127w, 1088w, 971w, 906w, 834w, 818m, 769w, 732m, 680w, 653m. *Anal.* Calc. for $C_{48}H_{48}N_{12}S_6Cu_3Br_6$: C, 34.83; H, 2.92; N, 10.15. Found: C, 34.62; H, 2.58; N, 10.45%.

2.4. X-ray crystallography

Diffraction intensity data for **1**–**4** were collected at 298(2) K with a Bruker SMART CCD-4K diffractometer by employing graphite-monochromated Mo Kα radiation (λ = 0.71073 Å). The data